Targeting Uropathogenic *Escherichia coli*, a Virulent Stains of Urinary Tract Infection: *In silico* Study of Aloe Barbadensis Miller Phytoconstituents

Mikidadi S. Gurisha [a*], P.V.Kanaka Rao [a] and Laxmikanth Cherupally [a]

[a] *Department of Physics, College of Natural and Mathematical Sciences, University of Dodoma P. O. Box 338 Dodoma, Tanzania.*

Authors' contributions

This work was carried out in collaboration among all authors. All authors read and approved the final manuscript.

Original Research Article

ABSTRACT

The most frequent pathogen linked to the development of UTIs is Uropathogenic *Escherichia coli* (UPEC). Thus, inhibiting the UPEC protein target (PDB ID 8BVD) would be a viable treatment approach. This study used molecular docking and dynamics to investigate *Aloe barbadensis* miller antibacterial activity against UPEC bacteria. The Phytoconstituents of *Aloe barbadensis* miller such as aloe-emodin, cholic acid, and flavonol were downloaded from the PubChem database with nitrofurantoin as a control drug and investigated against the target molecule. Some potential parameters such as docking scores, absorption, distribution, metabolism, excretion, toxicity (ADMET), oral bioavailability, root mean square deviation (RMSD), root mean square fluctuation (RMSF), hydrogen bonding, radius of gyration, and total energy of the system were examined.

_____

Corresponding author: E-mail: salehegs@gmail.com;

According to the docking score results, all ligands showed excellent candidacy as an inhibitor of the 8BVD molecule. The score order was aloe-emodin (-6.6 kcal/mol), cholic acid (-6.8 kcal/mol), flavonol (-6.8 kcal/mol) and nitrofurantoin (-6.1 kcal/mol). Every ligand seemed to possess favorable drug-likeness characteristics and oral bioavailability. Molecular dynamics investigation showed that every ligand demonstrated a strong candidate for an inhibitor in its vicinity of 20 ns. Contrary to cholic acid, which appears to be more stable, aloe-emodin and flavonol showed comparatively high fluctuations. The results of this study imply that the chosen Phytoconstituents may be employed as 8BVD protein inhibitors to combat urinary tract infections. Nevertheless, the room is still available for more research to validate the particular mechanism of UTI treatment through clinical and experimental methods.

Keywords: Molecular docking; Molecular dynamics; Phytoconstituents; Uropathogenic; Escherichia coli; Virulent strain.

1. INTRODUCTION

Urinary tract infection (UTI) is the most prevalent infectious disease identified worldwide, particularly in many developing countries [1]. It is one of the predominant microbial disorders in clinical practice. Approximately 150 million people are believed to have UTIs globally with significant morbidity and high medical costs per annum [2]. The annual societal costs of these infections in the USA alone are estimated to be around US dollar 3.5 billion, including medical expenses and lost productivity [3]. Most of the population visiting healthcare facilities, especially those in developing and middle-income countries, perceived the disease more often. This includes schoolchildren, students in higher learning institutions, and any member of the public, mostly women living in communal camps or organizations. There are two clinical classifications for UTIs; complicated and non-complicated types. "Several factors that impair the urinary tract or host defense have been connected to complicated UTIs including immunosuppression, renal failure, pregnancy, urinary blockage, urine retention, and indwelling catheters or other drainage, while non-complicated UTIs were associated with the health of patients showing the absence of structural or neurological urinary tract abnormalities" [3,2].

Uropathogenic E. coli (UPEC) is a major cause of UTIs leading to a significant burden on public health [4]. UPEC are the most commonly isolated bacteria globally accounting for 80 to 90%, compared to other gram-negative and gram-positive bacteria [5 & 6]. "The bacteria have stains that change from their commensal state as intestinal flora develop and remain in the urinary tract, and exhibit a wide range of virulence factors and tactics, allowing them to infect and cause illnesses in the urinary tract" [7].

Antibiotics such as nitrofurantoin, β-lactams, trimethoprim, and quinolones have been used as routine treatments of UTIs in many developing countries. Although some of these medications have been shown to be effective in reducing the clinical symptoms of UTIs, recurring and chronic infections still affect many individuals [8]. "Phytochemicals derived from natural products have been used in drug development, and these products have been considered in the chase for the novel medication combined with other strategies like computational method" [9].

"Computational methods of molecular docking and dynamics are effective for identifying new drugs and are thus widely used in the pharmaceutical industry" [10]. "Computer-aided drug discovery and design may shorten the time taken for a medicine to reach the consumer market, in addition to lowering the expenses involved in drug discovery by guaranteeing that the best lead molecule can enter animal trials" [11].

"Medical plants with antibacterial and anti-inflammatory qualities have been used recently to treat a wide range of infectious diseases in humans" [12]. "Aloe vera (*Aloe barbadensis miller*) is a well-known therapeutic plant used against UPEC" [13]. "Its phytoconstituents have major pharmacological features and are widely recognized for their numerous health benefits including its ability to boost immunity, reduce inflammation, prevent sunburn, age prematurely, and anti-cancer" [14]. "As a result, they are becoming increasingly popular among clinical researchers as a way to provide cost- and time-efficient therapeutic options for eradicating UTIs" [14 &15].

Therefore, this study used computational methods to ascertain the antibacterial properties of aloe-emodin, cholic acid, and flavonol derived from *Aloe barbadensis miller* and nitrofurantoin as control drugs. Molecular docking and dynamic studies were conducted to evaluate important parameters such as docking score, hydrogen bond, root mean square deviation (RMSD), root mean square fluctuation (RMSF) radius of gyration, and total energies of the system*.*

2. MATERIALS AND METHODS

2.1 Materials Collection

The structures of aloe-emodin, cholic acid, flavonol, and nitrofurantoin were downloaded from the PubChem library as 3D conformers and saved as a structure data file (sdf) [16].Their molecular structures are shown in (Fig 1).

2.2 Protein Selection and Preparation

"The protein molecule UPEC type 1 fimbrial (FimH) lectin domain in complex with mannose C-linked to quinolone was downloaded from Protein Data Bank (PDB ID: 8BVD)" [17]. "Using the X-ray diffraction method the desired macromolecule was obtained with a resolution of 3.00 Å an R-value free of 0.303 and an R-value work of 0.251, indicating good quality and high resolution of the molecule" [18]. "UPEC type 1 FimH complex molecules are desirable substitutes for antibiotic therapy and prophylactic measures against acute or urinary tract infections" [4 & 19]. Protein receptors were prepared using the Usf Chimera software by removing solvent and ligand molecules from the 8BVD target, removing residues selenomethionines to methionine's, adding hydrogen atoms, and charging the protein for protein optimizations [20]. For site-specific docking, the ligand coordinates for the center at X: 26, Y: 58, Z: -9, and box with dimensions of X: 13, Y: 7, and Z: 10 were designed. The ready-to-dock protein receptor was saved in the mol2 file.

2.3 Ligand Preparations

The Phytoconstituents of *Aloe barbadensis miller* were recovered from the commercial PubChem library that was easily accessible. The ligands were prepared using Ucsf Chimera software, which optimized them to match the protein and saved the results as mol2 in the working directory [21].

2.4 Molecular Docking

Docking is a computational technique that forecasts the interaction between small molecules (ligands) and proteins (enzymes). The program's score function analyzes the docking results; a lower value indicates a better interaction [22]. Molecular docking was performed using Ucsf chimera software that can be expanded upon to facilitate the interactive conception and investigation of molecular structures and associated data. This includes sequence alignments, density maps, conformational ensembles, docking results, trajectories, and supramolecular assemblies [23].

"The protein receptor and the minimized ligand saved in the mol 2 file were selected and opened in the auto dock vina window. The receptor and ligand were selected as outputs, and the coordinates for the center and the size for site-specific docking were generated in the boxes. The executable location path for the vina and vina splits was set and docking was performed" [24].

2.5 Physicochemical, Pharmacokinetics, Drug-Likeness and ADMET Prediction

The pharmacokinetic and pharmacodynamic profiles of a drug are largely determined by its physicochemical qualities, which are crucial for boosting a drug candidate's chances of success during the preclinical development process [25]. Drug candidates fail in clinical trials for a variety of reasons, but the two main reasons are undesirable pharmacokinetic characteristics and unacceptable toxicity [26]. Drug candidates must thus be chosen carefully by researchers to ensure that effectiveness, absorption, distribution, metabolism, excretion, and toxicity are all balanced [27]. On the other hand, certainly, the inhibition of these isoenzymes (CYP1A2, CYP2C19, CYP2C9, CYP1A2, CYP2D6, and CYP3A4) contributes to pharmacokinetics. Related drug-drug interactions can result in toxic or other unfavorable side effects because of the reduced clearance and buildup of the drug or its metabolites. In this study, the three best-scoring ligands were evaluated: physicochemical, pharmacokinetic (PK), Drug-Likeness and ADMET Prediction using pkCSM and SwissADME web tools [28, 29].

2.6 Bioavailability Radar

"Drug likenesses are quickly assessed by using bioavailability radar, in this case, six physiochemical parameters like lipophilicity, size, polarity, solubility, flexibility, and saturation were

considered" [30]. SwissADME software was used to conduct thorough and accurate testing [29 & 30].

2.7 Molecular Dynamics

"The GROMACS software was used to perform molecular dynamics simulations on 8BVD-CID10207, 8BVD-CID221493, 8BVD-CID11349, and 8BVD-CID6604200 at 300 K with a CHARMM27 force field, and the hybrid ligand structure and force field properties of the chosen ligand were determined using Swiss Param" [31].

"Free 8BVD, 8BVD-CID10207, 8BVD-CID221493, 8BVD-CID11349, and 8BVD-CID6604200 were solvated with water in a cubic box with a basic diameter of 1 nm with all default settings. Using constant volume and periodic boundary conditions, the system temperature was raised from 0 to 300 K throughout the equilibration time (1000 ps). The system was then lowered using the 1000 sharpest decline steps. The created trajectories were utilized to evaluate each complex's behavior as well as the system's overall stability. Calculations of the hydrogen bond, root mean square deviation, root mean square fluctuation, radius of gyration, and total energies were used to examine the variations in the macromolecule and macromolecule-ligand complex system" [32].

The equilibration process was divided into two phases using the number of particles, system volume and temperature (NVT) ensemble, and number of particles system pressure and temperature (NPT) ensemble. The C backbone atoms of the original structures were confirmed, while all the other atoms were free to move in both NVT and NPT. Molecular dynamics (MD) was then run at 300k with a 20ns time frame. The GROMACS analysis modules were used to examine the trajectories obtained. UCF Chimera and Maestro were used to visualize MD movies and interaction diagrams, respectively [33].

3. RESULTS AND DISCUSSION

3.1 Docking Scores

Molecular docking scores for aloe-emodin, cholic acid, flavonol, and nitrofurantoin are shown in Table 1. According to the scores, the ligand cholic acid has the lowest affinity for binding to the 8BVD target. A lower docking score indicates that ligand and target binding are more stable. The different structures bound to the target caused variations in ligand-target interactions which led to different docking scores [10, 33] (Fig 2). Small molecules of cholic acid have been reported as potential lead drugs for the treatment of bacterial infections [34].

(a)

(b)

(c)

(d)
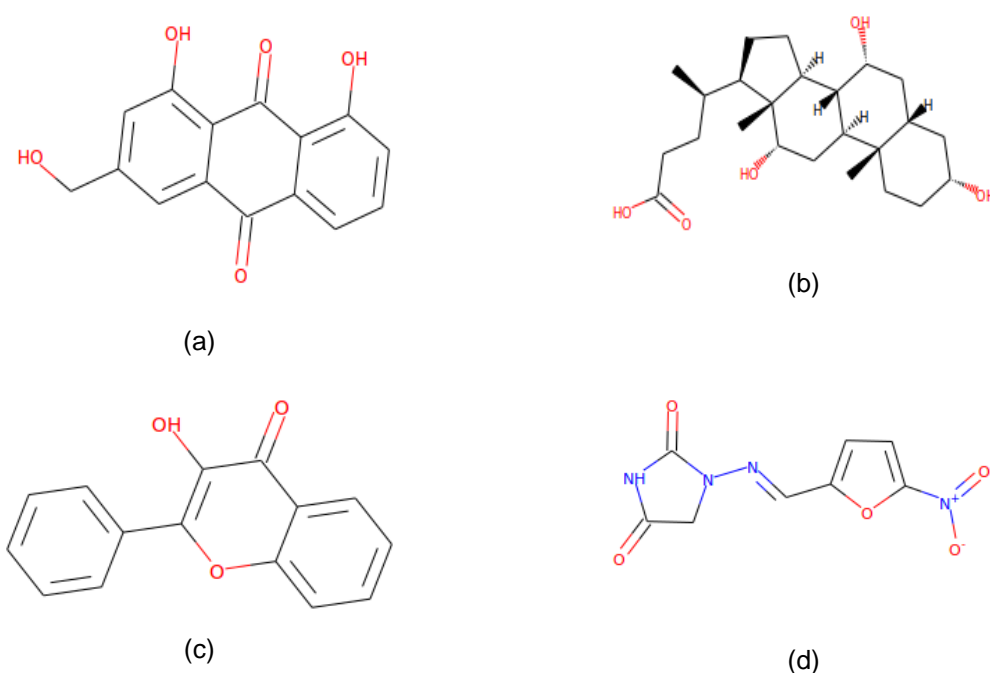
Fig. 1. Molecular structures of the compounds (a) aloe-emodin, (b) cholic acid, (c) flavonol and (d) nitrofurantoin

3.2 Physicochemical, Pharmacokinetics, Drug-Likeness and ADMET Prediction

A molecule needs to have the ideal pharmacokinetics and safety profile in addition to the intended biological functions to be taken into consideration as a potential therapeutic candidate [35]. One of the biggest challenges for oral medicine is its ability to cross the intestinal epithelial barrier, which affects the rate and degree of human absorption [36]. The selected compounds have an intestinal absorption rate of more than 60%, which is extremely high (Table 2). The selected molecules are non-hepatotoxic, do not cause skin sensitization, are non-permeable to the central nervous system (CNS) and blood-brain barrier (BBB), and exhibit negative AMES toxicity. It can also be reported that all ligands in this assessment permeate colon carcinoma cell 2 (CaCo-2) although aloe-emodin seems to have a low penetration potential.

The metabolic enzyme cytochrome P450 (CYP450) was examined and tested in the context of metabolism. The results indicating that, aloe-emodin and flavonol are potential inhibitors of CYP1A2, CYP1A2, and CYP3A4. Every ligand was also examined for toxic risks, such as hepatotoxicity, and the findings demonstrated that none of the substances could harm or impair the liver (Figure 2). The combination of the drug-likeness and ADMET properties suggested that aloe-emodin, flavonol, and cholic acid could be good options to inhibit the target in UTI drug development. According to the available data, aloe-emodin has a wide range of pharmacological effects such as anti-inflammatory, antibacterial, neuroprotective, hepatoprotective, and anti-tumor effects [37]. Cholic acid has been described to exhibit antibacterial, anti-viral, anti-fungal, anti-malaria, anti-tubercular, anti-tumor, and anti-allergic. It is a useful building block that can be used to create new molecules and a variety of compounds [38].
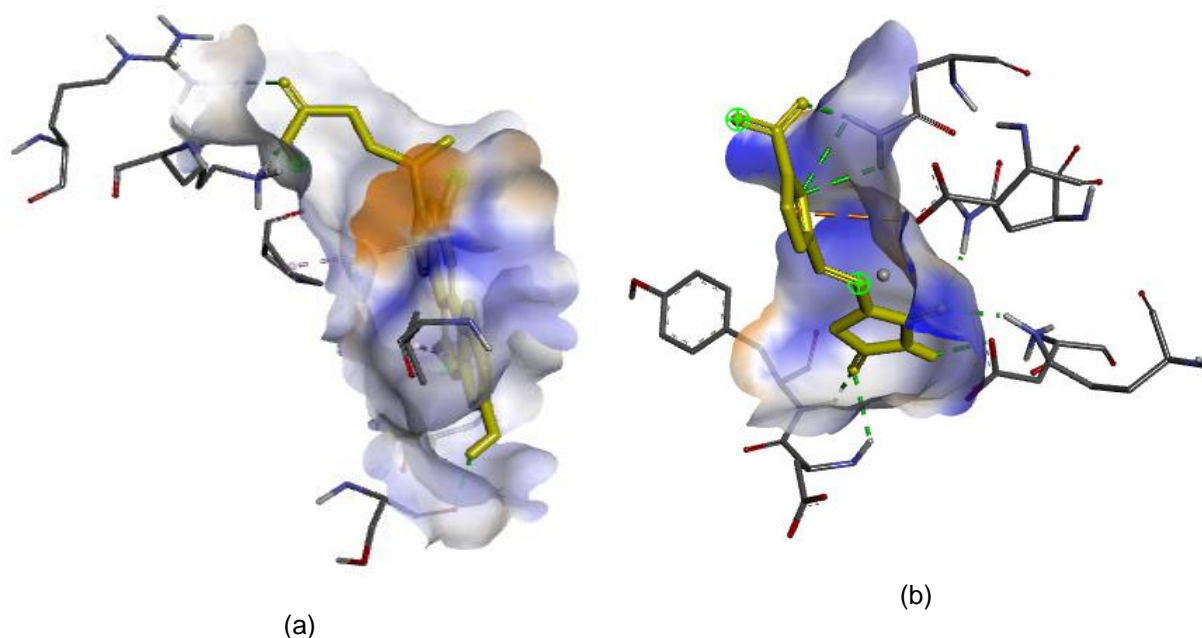

(a)

(b)

Fig. 2. Visualization of hydrophobic interaction between 8BVD with cholic acid ligand (a) and (b) nitrofurantoin

Table 1. Docking score for ligand-protein targe

PubChem ID	Molecular Formula	Name	Docking Scores (kcal/mol)
10207	$C_{15}H_{10}O_5$	Aloe-emodin	-6.6
221493	$C_{24}H_{40}O_5$	Cholic Acid	-6.8
11349	$C_{15}H_{10}O_3$	Flavonol	-6.7
6604200	$C_8H_6N_4O_5$	Nitrofurantoin	-6.1

Table 2. ADMET prediction of the highest scoring Phytoconstituents

Properties	Model Name	Predicted Value				
		CID 10207	CID 221493	CID 11349	CID 6604200	Unit
Absorption	Water solubility	-3.104	-3.763	-3.683	-2.906	mol/L
	P-gp substrate	No	Yes	No	No	-
	P-glycoprotein	No	Yes	No	No	-
	Gastrointestinal absorption	High	High	High	High	-
	Caco-2 permeability	-0.233	0.597	1.263	-0.013	cm/s
	Intestinal absorption(%	74.179	61.546	94.776	79.533	-
Distribution	BBB permeability	-0.729	-0.716	0.462	-0.9	Log BB
	VDss (human)	0.671	-0.804	0.214	-0.544	Log L/kg
	Fraction unbound	0.226	0.171	0.151	0.54	Fu
	CNS permeability	-0.2466	-2.344	-1.733	-3.18	Log Ps
	Leadlikeness	Yes	No	No	No	-
Metabolism	Inhibitor	Yes	No	Yes	No	-
	CYP1A2	No	No	Yes	No	-
	CYP2C19	No	No	No	No	-
	CYP2C9	No	No	Yes	No	-
	CYP2D6	Yes	No	Yes	No	-
	CYP3A4 CYP1A2	Yes	No	Yes	No	-
Excretion	Total Clearance	0.008	0.653	0.233	0.665	ml/min/kg
	Renal OCT2 substrate	No	No	No	No	-
Toxicity	Skin sensitization	No	No	No	No	-
	Hepatotoxicity	No	No	No	No	-
	AMES toxicity	No	No	No	Yes	-

Flavonol is a ketone group of flavonoid [39]. They are considered antioxidant, anti-mutagenic, anti-inflammatory, and anti-carcinogenic. In addition to these abilities, they also alter the activities of important cellular enzymes [40].

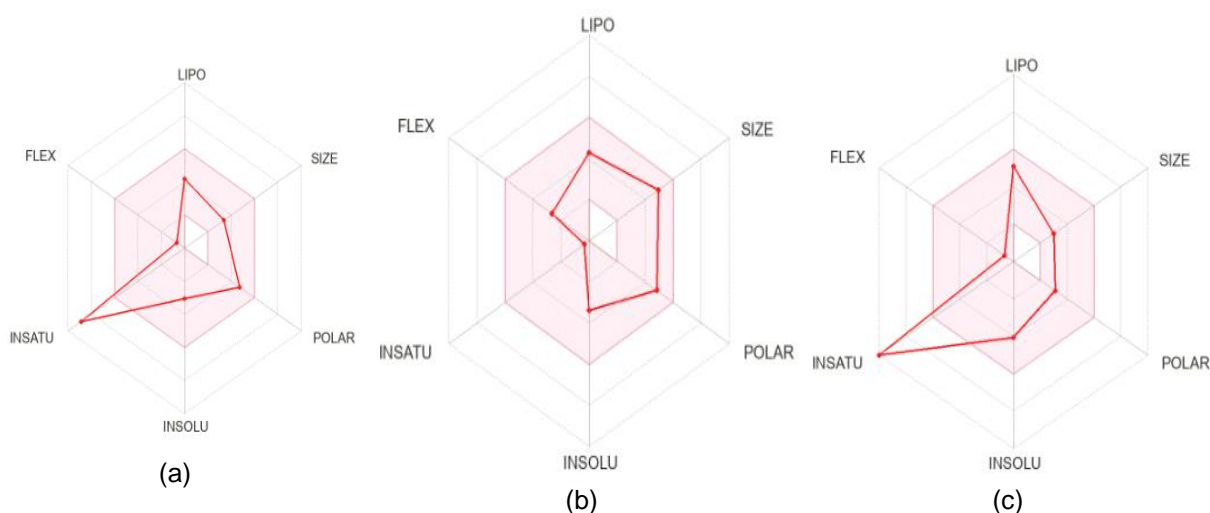## 3.3 Bioavailability Radar

A molecule's radar plot needs to fall inside the colored zone to be considered drug-like (Fig 3). For each variable, the pink zone indicates the proper range, such as lipophilicity: XLOGP3 range between -0.7 to 5.0, molecular weight (Mw) ranges between 150 and 500 g/mol, topological polar surface area (TPSA) ranges between 20 and 130 Å², solubility: logS less than 6, saturation (INSATU): fraction csp3 hybridization fraction greater than 0.25, and

flexibility: less than 9 rotatable bonds (Table 3). Therefore, based on the bioavailability radar indicated in Figure 3, cholic acid has oral bioavailability, while aloe-emodin and flavonol appear to be more unsaturated with respect to carbon percentage in sp3 hybridization.

To conduct visual analysis, the positions for every ligand-target interaction were compared. To facilitate ligand interactions, the protein active sites were created. Initially, the analysis of the aloe-emodin-target, in which its 2D projection interaction is displayed in Fig 4(a), was deliberated. The three OH groups in aloe-emodin form hydrogen bonds with protein residues Asp47, Asp54, Asp140, Gnl133, and Phe1. In this case, aloe-emodin acts as a hydrogen donor

Table 3. Phytoconstituents and drug-like properties analysis

Descriptor/Properties	Value				
	CID 10207	CID 221493	CID 11349	CID 6604200	Units
Molecular Weight	270.24	408.6	238.24	238.16	g/mol
Monoisotopic Mass	270.052826	408.287567	238.062994	238.033813	Da
Rotatable Bonds	1	4	1	3	-
H. Acceptors	5	5	3	6	-
H. Donors	3	4	1	1	-
LogP	1.3655	3.4487	3.1656	0.0735	-
Num. arom. heavy atoms	12	0	16	5	-
Fraction Csp3	0.07	0.96	0.0	0.12	-
Num. of heavy atoms	20	29	18	17	
Topological Polar Surface Area	94.83	97.99	50.44	120.73	Å²
Molar Refractivity	69.92	113.76	69.94	62.8	-

(a)   (b)   (c)

Fig. 3. Bioavailability radar of (a) aloe-emodin, (b) cholic acid and (c) Flavonol

to the polar residues Asn54 and Asp140, whereas it acts as an acceptor to the amino acid residues Asp47, Gln133, and Phe1. The bond formed here is somewhat complicated, where aloe-emodin acts as a hydrogen donor and acceptor simultaneously.

The second pose is the cholic acid-target interaction, as displayed in Fig 4(b). The figure shows that cholic acid forms two OH groups in the form of hydrogen bonds with Asp140, and two oxygen bonds with Asp47 and Phe1. In this case, the Asp140 polar residue acts as a hydrogen acceptor, while the amino acid residues Asp47 and Phe1 act as donors to cholic acid oxygen atoms. It is estimated that the docking score of cholic acid is more negative than that of aloe-emodin owing to the interaction

of two hydrogen bonds with the Asp140 polar residue.

The third pose is the flavonol-target interaction, as displayed in Fig 4(c). The figure illustrates that flavonol forms one OH group in the form of a hydrogen bond with Asp140 and one oxygen bond with Asn138. In this case, the Asp140 polar residue acts as a hydrogen bond acceptor, whereas Asn138 acts as a donor to a flavonol oxygen atom. In this situation, the docking score of flavonols seems to be more negative than that of aloe-emodin.

The fourth pose is the nitrofurantoin-target interaction, as displayed in Fig 4(d). This figure indicates that nitrofurantoin forms a hydrogen bond with Asp54 and an oxygen bond with

Asp47, Asn135, Gnl133, and Tyr48. In this case, the Asp54 polar residue acts as a hydrogen acceptor, while Asp47, Asn135, Gnl133, and Tyr48 act as donors to a nitrofurantoin oxygen atom. In this phenomenon, the docking score of nitrofurantoin appears to be less negative than flavonol compounds.

In general, the complexity of protein-ligand interactions determines the strength of molecular docking [41]. Aloe-emodin has hydrogen bonds with Asp47, Asp54, Asp140, Gnl133, and Phe1which are more complicated than those of cholic acid, which has two hydrogen bonds with Asp140, flavonol, and nitrofurantoin, which have a single hydrogen bond with Asp140 and Asp54, respectively. Therefore, from the visual analysis, the best compound to form a ligand target was cholic acid, followed by flavonol, aloe-emodin, and nitrofurantoin, which were endorsed by the protein-ligand interaction docking scores (Table 1).

Nitrofurantoin has become the first-line drug choice for the treatment of uncomplicated UTIs in light of updated guidelines, and its use has skyrocketed since then [42]. From the docking results, nitrofurantoin has a more positive value of the docking score compared with the other three ligands although both have good hydrogen bond interactions. Having the more negative value of the docking scores of aloe-emodin, cholic acid, and flavonol suggests that they might be a suitable candidate for the treatment of UTIs in comparison with the control drug.

3.4 Molecular Dynamics

Molecular dynamics is a computer modeling technique that forecasts the motion of each atom in a protein or other molecular system over time [43]. It provides an overview of the system dynamics evolution.

Molecular dynamics (MD) was performed to examine the actual motion of atoms, which aids in understanding the detailed interaction of 8BVD with potential phytochemicals, especially when it binds to a protein target [44]. Several non-identified biological activities and intricate dynamic processes can be discovered by observing the internal dynamics of proteins [45].

3.5 Hydrogen Bonding (H-Bonds) Analysis

The stability of a protein's three-dimensional structure is mostly determined by intramolecular

hydrogen bonding within the protein molecule [46]. Hydrogen bond analysis can also be used to examine the strength of the protein-ligand complex to assess the molecular recognition, directionality, and specificity of contacts [47]. The analysis showed that aloe-emodin formed a maximum of 6-H bonds during the molecular dynamics computation. It was observed that aloe-emodin binds to the active pocket of 8BVD with many H-bond breakages from five to six H-bonds. From 0 to 4 ns, 1 to 5 hydrogen bonds were formed with bond breaking. From 5 to 13 ns, there were one to two stable H-bonds with fluctuations, followed by bond breaking from 13 to 18 ns. Again, from 18 to 20 ns, stable hydrogen bonds were formed, with some fluctuations (Fig 5 a).

Cholic acid formed a maximum of six H-bonds during the molecular dynamic computation. From 8 to 16 ns, a 1–2 H-bond was formed by bond breaking. From 0 to 20 ns, cholic acid bound to the active pocket of 8BVD and formed two to four H-bonds, which were the most stable, although there were some fluctuations. Stable H-bonds were formed between 4 and 5.

Hydrogen bonds with high fluctuations compared to the H-bonds formed between 2 two four H-bonds. Equally, from 5 to 6, hydrogen bonds were formed with bond breaking (Fig 5 b).

Molecular dynamics analysis revealed that flavonol binds to the active pocket of 8BVD and forms a 3 H-bonds. From 0 to 1ns, 0.5 to 2 H-bonds were formed, with some bond breakage. Equally, 0.5 to 3 H-bonds were formed with fluctuations and bond breakage from 2 to 7 ns. From 9 to 16 ns there a 0.5 to 1 hydrogen bond was formed with bond breakage (Fig 5 c).

Nitrofurantoin was observed to form a maximum of five H-bonds during the molecular dynamic simulation. From 12 to 20 ns, nitrofurantoin formed a 1H-bond with fluctuations and bond breakage. Similarly, 1 to 2 H-bonds were formed with some fluctuations and bond breakage, especially from 2 to 12 ns and 16 to 20 ns. Nitrofurantoin formed stable hydrogen bonds from two to four H-bonds with fluctuations and bond breakage, especially from 12 to 20 ns. Other hydrogen bonds were formed between four and five H-bonds with high fluctuations and bond breakage, particularly from 12 to 20 ns (Fig 5 d). Primarily, all four ligands had good H-bonding with the active pocket 8BVD; however, cholic acid had the most stable H-bonding in
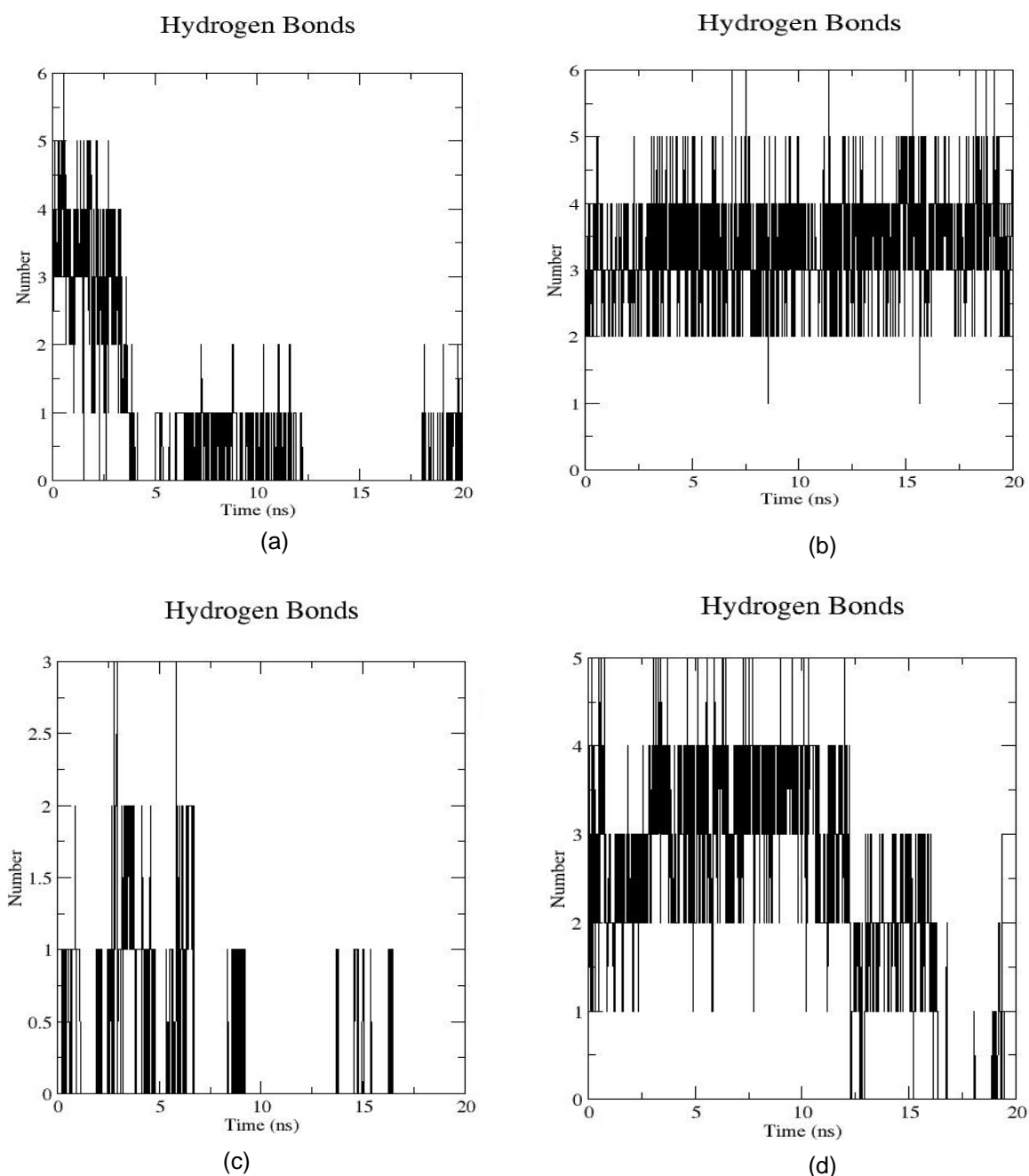
comparison to other ligands. Protein-ligand binding is highly influenced by H-bonding [48].

Therefore, cholic acid has excellent potential for use as a drug candidate.

(a)

(b)

(c)

(d)
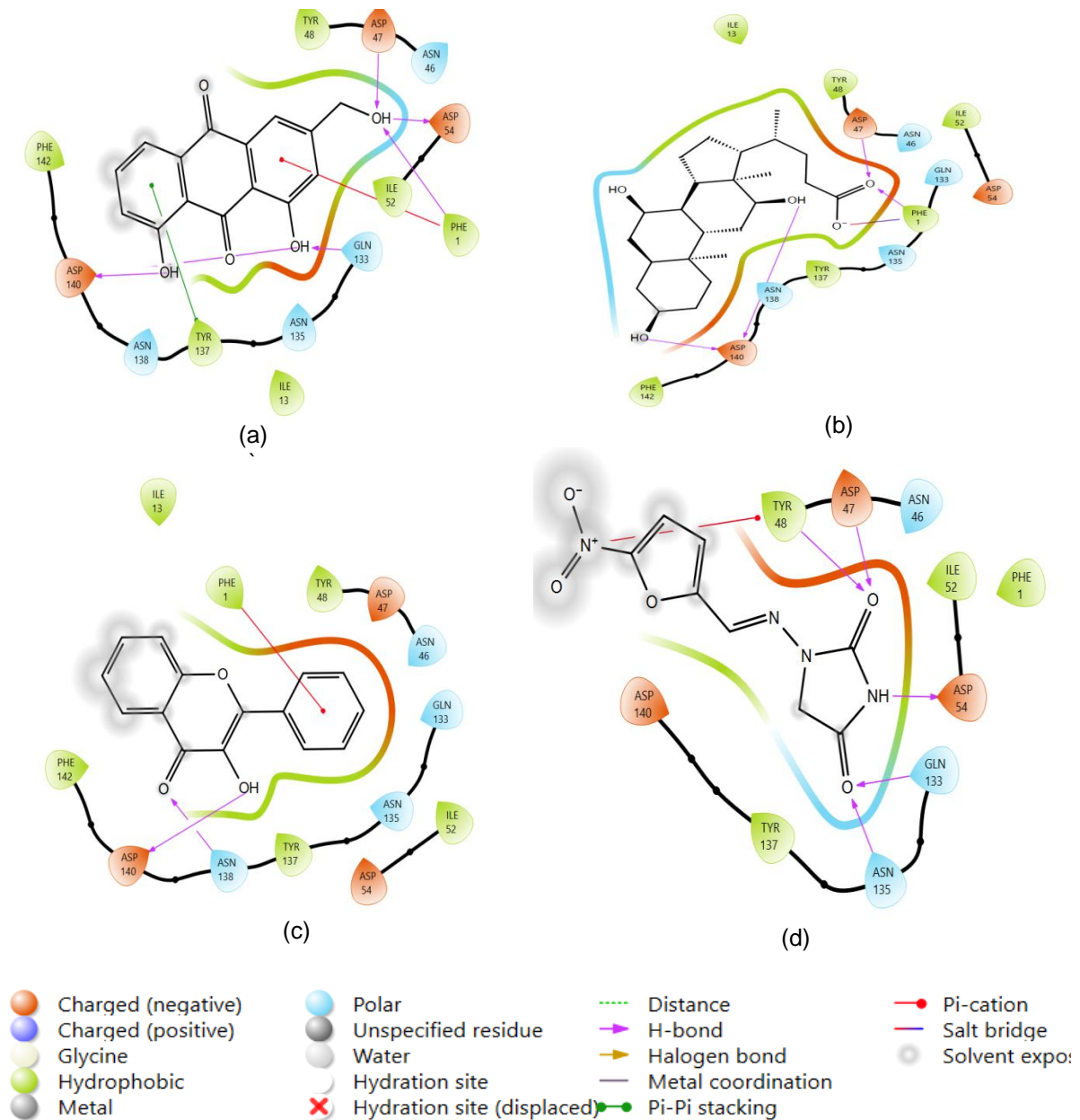
Fig. 4. Two-dimension interaction diagrams in various possess within the binding pocket 8BVD for (a) aloe-emodin, (b) cholic acid, (c) flavonol and (d) nitrofurantoin

Fig. 5. Hydrogen bonds formed by (a) aloe-emodin (b) cholic acid (c) flavonol and (d) nitrofurantoin

3.6 Root Mean Square Deviation (RMSD)

The root mean square deviation of each trajectory record for 20 ns in the MD simulation with regard to the initial position of the protein ligand was measured to assess the stability of the docked complex [49]. The mean RMSD for aloe-emodin was 2.32 nm. The plot showed that aloe-emodin binds effectively more stable with

8BVD at 0.99 nm from 0 to 12 ns, and then destabilized at 13 ns to 18 ns.

From the trajectory analysis, cholic acid appeared to bind more strongly with the target molecule at 0.8 nm. Initially, the ligand had a slight destabilization from 0–3 ns before stabilizing at 0.35 ns. The mean root mean square deviation (RMSD) was 0.620 nm.
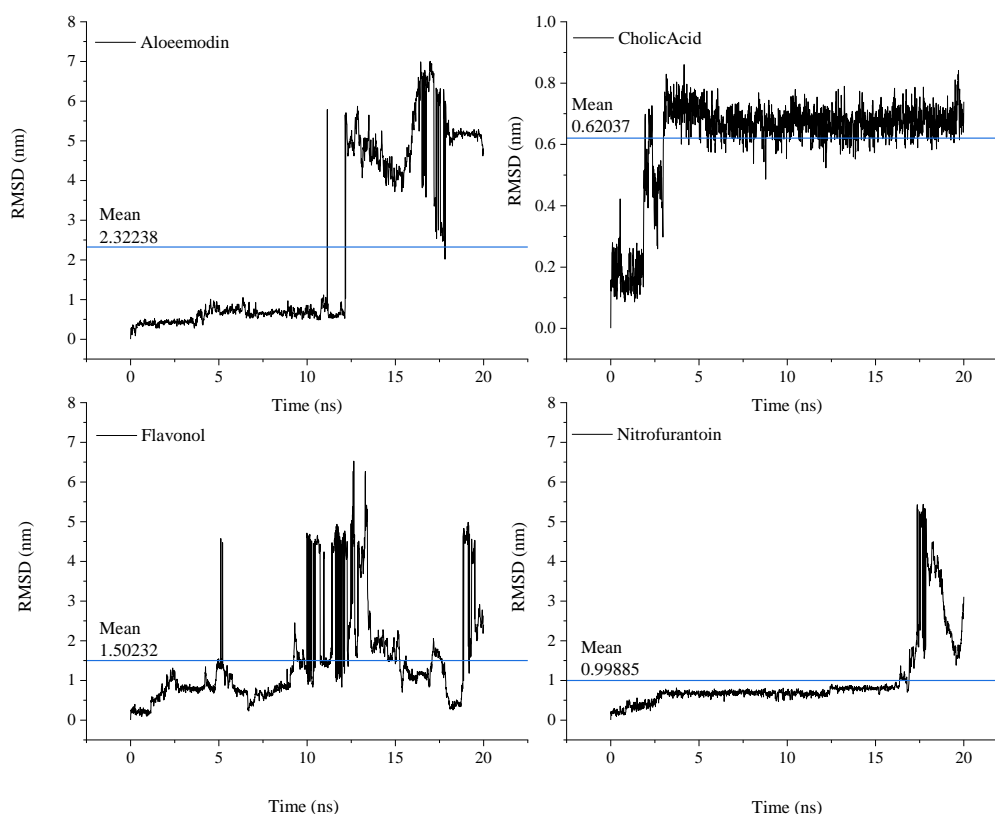
Fig. 6. RMSD for aloe-emodin, cholic acid, flavonol and nitrofurantoin ligands

The flavonol ligand was stable from 0–4 ns, before fluctuating at 5 ns. From 5.5 to 9.5 ns the ligand was re-stabilized, but then destabilized from 10 to 13 ns before gaining stability at 18 ns. The mean RMSD value was recorded at 1.50 nm.

RMSD for nitrofurantoin ligands was stable at 0.89 nm from 0 to 17 ns, and then destabilized from 18 ns up to 20 ns. The mean RMSD was recorded at 0.99 nm. Looking at their ranges, cholic acid had the lowest range followed nitrofurantoin, flavonol and aloe-emodin (Fig 6).

3.7 Root Mean Square Fluctuation (RMSF)

The flexibility of each amino acid residue, or how much it shifts or fluctuates throughout a simulation, was measured by root mean square fluctuation (RMSF), which averages the number of atoms to determine how far an atom or group of atoms has deviated from the reference structure. According to literatures, stable structures have lower RMSF values [10, 49]. The fluctuation of different atoms was observed for 20 ns, to predict the stable structure, and the RMSF

was computed using the GROMACS standard function. The analysis shows that the H10 atom of aloe-emodin fluctuated more than the other atoms. The RMSF value of the H10 atom was 0.151 nm, followed by HC5 and HC6, both with RMSF value of 1.121 nm. O5, H8, and H9 atoms fluctuated at an RMSF value of 0.102 nm while the HO atoms fluctuated at 0.7 nm. The other atoms were stable at an average RMSD value of 0.03 nm (Fig 7 a).

The HC31 atom of cholic acid was perceived to have the highest fluctuation at an RMSF value of 0.186 nm, followed by HC32 and HC30 with RMSF values of 0.183 and 0.182 nm, respectively. O5, C22, and HC23 exhibited RMSF values of 0.14, 0.13 and 0.13 nm respectively. The other atoms are stable at an average RMSF value of 0.065 nm (Fig 7 b).

For the case of flavonol, the HC7 atom seems to have a higher fluctuation at an RMSF value of 0,225 nm followed by HC8 fluctuating at 0.221 nm. Both HC4 and HC5 fluctuated at the RMSF value of 0.212 nm while C14 fluctuated at 0.151nm. C10 fluctuated at the RMSF value 0f 0.150 nm followed by C9 and C13 both

fluctuated at 0.149 nm. Other atoms are stable at an average RMSF value of 0.499 nm. (Fig 7 c)

In the case of nitrofurantoin, the HC7 atom had a higher fluctuation with an RMSF value of 0.209 nm, followed by HC8, HC4, and HC5 atoms with RMSF values of 0.207, 0.205, and 0.204 nm, respectively. In contrast, atoms such as C14, C13, C9, C10, and H10 also fluctuated, with RMSF values of 0.125, 0.123, 0.122, 0.123, and 0.121 nm, respectively. The other atoms appear to be stable at an average RMSF value of 0.320 nm (Fig 7 d). Most of the atoms observed to have higher RMSF values were terminal atoms.

3.8 Radius of Gyration (Rg)

The compactness of a protein structure is determined by its radius of gyration. In the protein-ligand complex, the radius of gyration of a ligand shows the ligand center of gyration to the center of gyration of the protein; therefore, a higher value of the radius of gyration indicates less stability of the structure [50]. From the analysis, it was observed that cholic acid gyrated more, with a higher value of 0.435 nm. This higher value is attributed to the higher molecular weight of cholic acid which is 408.6 g/mol and the complex shape of the ligand [51].

Flavonol had the lowest Rg value of about 0.315 nm at 20 ns. The ligand gyrated with this lower value because of the simple structure of flavonol and its lower molecular weight compared to cholic acid. Other ligands such as aloe-emodin and nitrofurantoin have a minimum value of Rg ranging from 0.330 to 0.380 nm respectively at 20 ns (Fig 8).

3.9 Total Energies of the System

The quality and stability of the molecular dynamic simulations were also evaluated through a qualitative investigation of the thermodynamic properties, such as the total energies and temperature [45, 51]. The temperature fluctuation of the trajectory was almost constant at 300 K, indicating the stable and precise nature of the molecular dynamics simulation. The total energies of the system of both proteins and ligands were plotted as a function of MD simulation time, and the plots are shown in Fig 9.
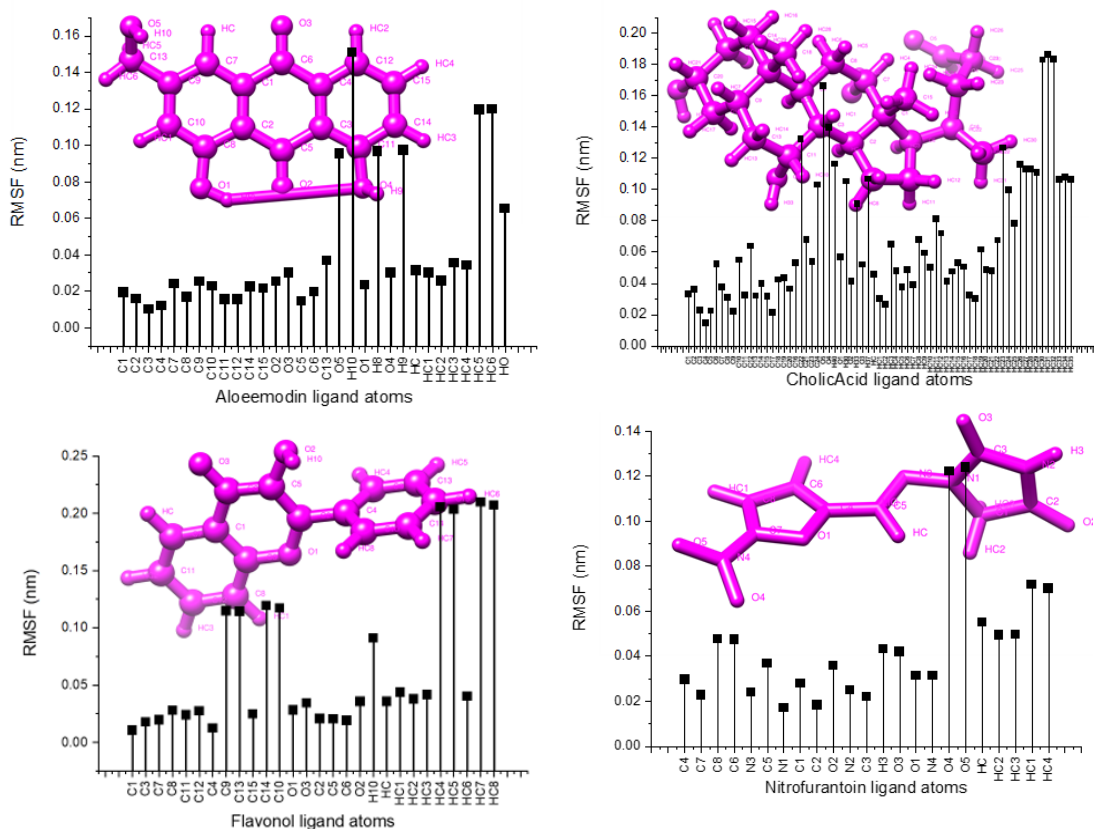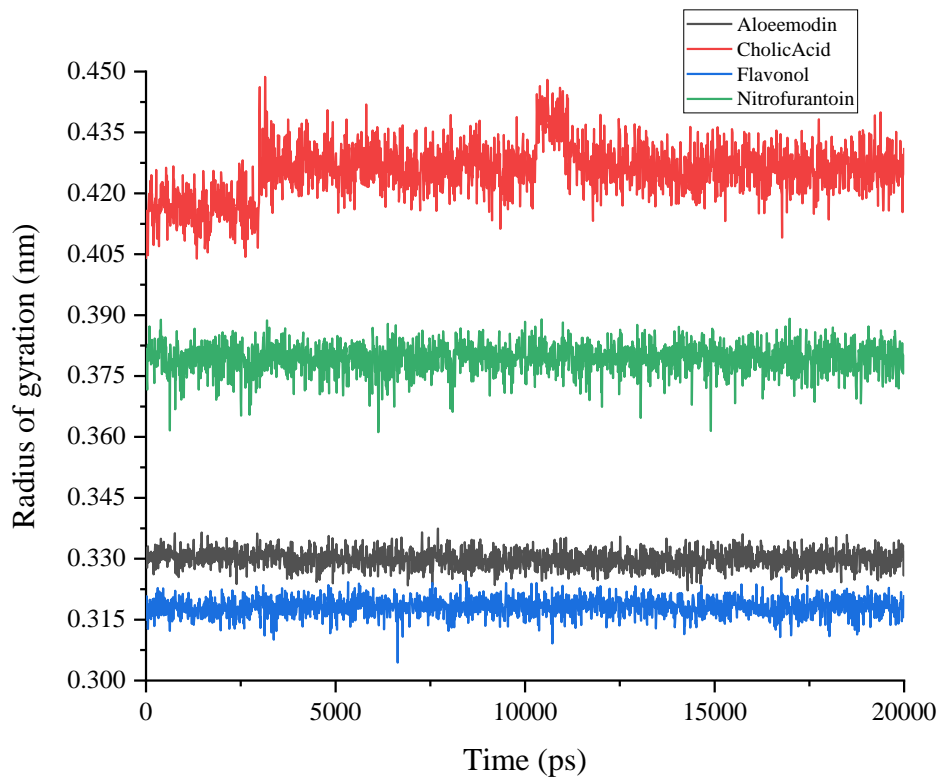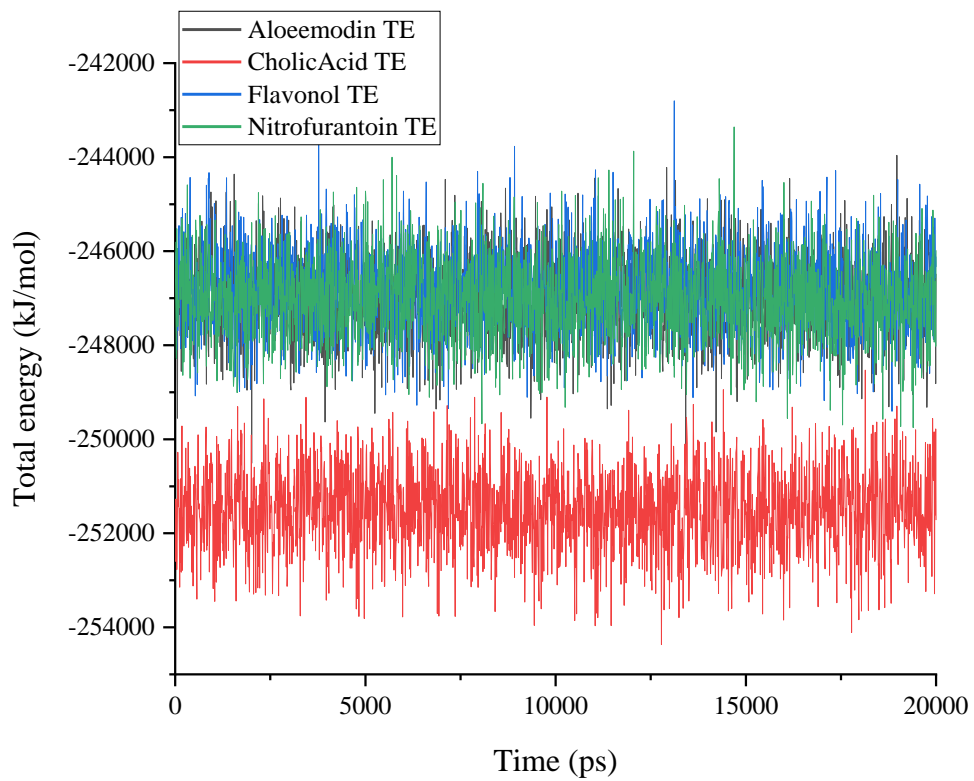

Fig. 7. RMSF for aloe-emodin, cholic acid, flavonol and nitrofurantoin ligands

Fig. 8. Radius of gyration for aloe-emodin, cholic acid, flavonol and nitrofurantoin ligands

Fig. 9. Total Energies of the system during the MD simulation

The results from the plot illustrate that cholic acid is more stable than the other three ligands, with a total energy of -252000 kJ/mol. Aloe-emodin, flavonol, and nitrofurantoin ligands were also stable, with slightly higher energies ranging from -248000 to -246000 KJ/mol. The trajectory profile's lower energy suggests that the system was remarkably stable during the simulation [52].

4. CONCLUSION

UPEC inhibition is an innovative approach for preventing the emergence of UTIs. Natural compounds are the most important source of medicines for the treatment of many diseases [53]. The ligand-target complex presented a good candidate for molecular docking and molecular dynamics. All ligands were superb candidates as 8BVD inhibitors based on the molecular docking scores, ADMET studies, and drug-like characteristics. Docking score ranges were arranged as follows from high to low as follows: cholic acid, flavonol, aloe-emodin, and nitrofurantoin. These results suggest that cholic acid is a more suitable inhibitor than other ligands. Molecular dynamics revealed that all ligands can also serve as excellent inhibitors, although fluctuations in aloe-emodin and flavonol remain high. However, additional studies and tests are required to validate these compounds as 8BVD protein inhibitors.

CONSENT AND ETHICAL APPROVAL

It is not applicable.

ACKNOWLEDGEMENT

COMPETING INTERESTS

Authors have declared that no competing interests exist.

REFERENCES

1. Beda John Mwang'onde, Josefine Innocent Mchami. The aetiology and prevalence of urinary tract infections in Sub-Saharan Africa: A Systematic Review, J. Health Biol Sci. 2022;10(1):1-7.

2. Zagaglia C, Ammendolia MG, Maurizi L, Nicoletti M, Longhi C. Urinary Tract Infections Caused by Uropathogenic Escherichia coli Strains-New Strategies for an Old Pathogen. Microorganisms. 2022 Jul 14;10 (7):1425.
DOI: 10.3390/microorganisms10071425

3. Flores-Mireles AL, Walker JN, Caparon M, Hultgren SJ. Urinary tract infections: Epidemiology, mechanisms of infection and treatment options. Nat. Rev. Microbiol. 2015;13:269–284.
DOI: 10.1038/nrmicro3432

4. Mousavifar L, Sarshar M, Bridot C. Scribano D, Ambrosi C, Palamara AT, Vergoten G, Roubinet B, Landemarre L, Bouckaert J. et al. Insightful Improvement in the Design of Potent Uropathogenic E. coli FimH Antagonists. Pharmaceutics. 2023; 15(2):527.
DOI: 10.3390/pharmaceutics15020527

5. Terlizzi ME, Gribaudo G, Maffei ME. UroPathogenic *Escherichia coli* (UPEC) Infections: Virulence Factors, Bladder Responses, Antibiotic, and Non-antibiotic Antimicrobial Strategies. Front Microbiol. 2017;(8):1566.
DOI: 10.3389/fmicb.2017.01566.

6. Seifu WD, Gebissa AD. Prevalence and antibiotic susceptibility of uropathogens from cases of urinary tract infections (UTI) in shashemene referral hospital, Ethiopia. BMC Infect Dis. 2018;18(1): 30.
DOI: 10.1186/s12879-017-2911-x.

7. Chhaya Shah, Ratna Baral, Bijay Bartaula and Lok Bahadur Shrestha. Virulence factors of uropathogenic Escherichia coli (UPEC) and correlation with antimicrobial resistance, BMC Microbiology Journal. 2019;19 (204).
Available:https://doi.org/10.1186/s12866-019-1587-3

8. Asadi Karam MR, Habibi M, Bouzari S. Urinary tract infection: Pathogenicity, antibiotic resistance and development of effective vaccines against Uropathogenic Escherichia coli. Mol Immunol. 2019;108: 56-67.
Available:https://doi.org/10.1016/j.molimm.2019.02.007

9. Haidan Yuan, Qianqian Ma, Li Ye and Guangchun Piao. The traditional medicine and modern medicine from natural products, review, MDPI Journal of Molecules. 2016;21:559.
DOI: 10.3390/molecules21050559

10. Fatriansyah JF, Rizqillah RK, Yandi MY, Fadilah, Sahlan M. Molecular docking and dynamics studies on propolis sulabiroin-A as a potential inhibitor of SARS-CoV-2. J King Saud Univ Sci. 2022;34(1):101707. DOI: 10.1016/j.jksus.2021.101707

11. Preman Geetika, Muskaan Mulani, Ayesha Bare, Khushboo Relan, Leebah Sayyed, Vikas Jha, Kavita Pandey. Screening of phytochemicals for anti-Tubercular potential using molecular docking approach. J Tuberc. 2022;5(1):1030.

12. Bittner Fialová S, Rendeková K, Mučaji P, Nagy M, Slobodníková L. Antibacterial activity of medicinal plants and their constituents in the context of skin and wound infections, considering european legislation and folk medicine-a review. Int J Mol Sci. 2021;22(19):10746. DOI: 10.3390/ijms221910746

13. Mehdi Goudarzi, Saeedeh Ghafari, Masoumeh Navidinia and Hadi Azimi. Aloe vera gel: effective therapeutic agent against extended-spectrum β-lactamase producing escherichia coli isolated from patients with urinary tract infection in Tehran-Iran, Journal of Pure and Applied Microbiology. 2018;11(3):1401-1408. Available:https://dx.doi.org/10.22207/JPAM.11.3.22

14. Maan AA, Nazir A, Khan MKI, Ahmad T, Zia R, Murid M, Abrar M. The therapeutic properties and applications of Aloe vera : A review. Journal of Herbal Medicine. 2018;12:1-10. DOI:10.1016/j.hermed.2018.01.002

15. Newman DJ, Cragg GM. Natural Products as Sources of New Drugs over the Nearly Four Decades from 01/1981 to 09/2019. J Nat Prod. 2020 Mar 27;83(3):770-803. doi: 10.1021/acs.jnatprod.9b01285.

16. Kim S, Chen J, Cheng T, Gindulyte A, He J, He S, Li Q, Shoemaker BA, Thiessen PA, Yu B, Zaslavsky L, Zhang J, Bolton EE. *PubChem 2023 update.* Nucleic Acids Res. 2023;51(D1): D1373–D1380. Available:https://doi.org/10.1093/nar/gkac956

17. Liebschner D., Afonine P.V., Baker M.L., Bunkóczi G., Chen V.B., Croll T.I., Hintze B., Hung L.W., Jain S., McCoy A.J., et al. Macromolecular structure determination using X-rays, neutrons and electrons: Recent developments in Phenix. *Acta Crystallogr. Sect. D Struct. Biol.* 2019;D 75:861–877. DOI: 10.1107/S2059798319011471

18. Gerard J, Kleywegt, Alwyn Jones T. Model building and refinement practice. In Methods in Enzymology. 1997;277:208-230. Available:https://doi.org/10.1016/S0076-6879(97)77013-7

19. Abe CM, Salvador A, Falsetti IN, Blanco E, Blanco M. Uropathogenic *Escherichia coli* UPEC) strains may carry virulence properties of diarrhoeagenic E. coli. FEMS Immunol. Med. Microbiol. 2008;52:397–406. DOI: 10.1111/j.1574-695X.2008.00388.x

20. Gurisha MS, Rao PVK, Cherupally L. (2024) Phytochemicals of Aloe barbadensis miller as Potential Inhibitors of Uropathogenic Escherichia coli for Urinary Tract Infection Therapy: An in Silico Approach. Open Jour nal of Biophysics. 2024;14:99-120. Available:https://doi.org/10.4236/ojbiphy.2024.142006

21. Pettersen EF, Goddard TD, Huang CC, Couch GS, Greenblatt DM, Meng EC, Ferrin TE. UCSF Chimera A Visualization System for Exploratory Research and Analysis. J. Comput. Chem. 2024;25(13): 1605-1612. Available:https://doi.org/10.1002/jcc.20084

22. Stanzione F, Giangreco I, Cole JC. Use of molecular docking computational tools in drug discovery. Progress in Medicinal Chemistry.2021;273–343. DOI:10.1016/bs.pmch.2021.01.004

23. Huang, C. C.; Couch, G. S.; Pettersen, E. F.; Ferrin, T. E. Pac Symp Biocomput 1996, 1, 724

24. Forli S, Huey R, Pique ME, Sanner MF, Goodsell DS, Olson AJ. Computational protein-ligand docking and virtual drug screening with the AutoDock suite. Nat Protoc. 2016 May;11(5):905-19. doi: 10.1038/nprot.2016.051

25. David Camp, Agatha Garavelas, and Marc Campitelli. Analysis of physicochemical properties for drugs of natural origin, J. Nat. Prod. 2015;78(6):1370–1382.DOI: 10.1021/acs.jnatprod.5b00255

26. Honório KM, Moda TL, Andricopulo AD. Pharmacokinetic properties and in silico ADME modeling in drug discovery. Med Chem. 2013;9(2):163-76. DOI: 10.2174/1573406411309020002.

27. Jia C-Yang, Li J-Yi, Hao G-Fei, Yang G-Fu . A drug-likeness toolbox facilitates ADMET study in drug discovery, Drug Discovery Today; 2019.

Available:https://doi.org/10.1016/j.drudis.2019.10.014

28. Pires DE, Blundell TL, Ascher DB. pkCSM: Predicting Small-Molecule Pharmacokinetic and Toxicity Properties Using Graph-Based Signatures. J Med Chem. 2015 May 14; 58(9):4066-72. doi: 10.1021/acs.jmedchem.5b00104.

29. Daina A, Michielin O, Zoete V. SwissADME: A free web tool to evaluate pharmacokinetics, drug-likeness and medicinal chemistry friendliness of small molecules. Sci Rep. 2017;7 (42717).Available:https://doi.org/10.1038/srep42717

30. Udugade SB, Doijad RC, Udugade BV. *In silico* evaluation of pharmacokinetics, drug-likeness and medicinal chemistry friendliness of momordicin1: An active chemical constituent of momordica charantia, J Adv Sci Res. 2019;10(3):222-229.

31. Van Der Spoel D, Lindahl E, Hess B, Groenhof G, Mark AE, Berendsen HJ. GROMACS: Fast, flexible, and free. J Comput Chem. 2005;26(16):1701-1718.DOI: 10.1002/jcc.20291

32. Salaria D, Rajan R, Mehta J, Awofisayo O,Olatomide A. Fadare,OA, Balvir K, Renato AC, Shikha RC, Neha K, Eun HC, Nagendra KK. Phytoconstituents of traditional Himalayan Herbs as potential inhibitors of Human Papillomavirus (HPV-18) for cervical cancer treatment: An In silico Approach. PLoS One. 2022;17(3):1-20.
Available:https://doi.org/10.1371/journal.pone.0265420

33. Walters JP, Rogers CM, Crago SP. Maestro software and application performance, Conference Paper, GOMACTech-14 conference; 2014.

34. Wu J, Yu TT, Kuppusamy R, Hassan MM, Alghalayini A, Cranfield CG, Willcox MDP.; Black DS, Kumar N. Cholic acid-based antimicrobial peptide mimics as antibacterial agents. Int. J. Mol. Sci.2022; 23:4623.
Available:https://doi.org/10.3390/ijms23094623

35. Hu Q, Feng M, Lai L, Pei J. Prediction of Drug-Likeness Using Deep Autoencoder Neural Networks. Front Genet. 2018;27 (9):585. DOI: 10.3389/fgene.2018.00585

36. Rao P, Shukla A, Parmar P, Rawal RM, Patel B, Saraf M, Goswami D. Reckoning a fungal metabolite, pyranonigrin A as a potential main protease (Mpro) inhibitor of novel SARS-CoV-2 virus identified using docking and molecular dynamics simulation. Biophys Chem. 2020;264: 106425. DOI: 10.1016/j.bpc.2020.106425

37. Dong X, Zeng Y, Liu Y, You L, Yin X, Fu J, Ni J. Aloe-emodin: A review of its pharmacology, toxicity, and pharmacokinetics. Phytother Res. 2020;34 (2):270-281. DOI: 10.1002/ptr.6532.

38. Tripathi Kishua, Kumar T. Siva. Antibacterial activity of organometallic complexes of cholic acid, Dige J of Nanomat and Biostr. 2010;5(3):763-770.

39. Panche AN, Diwan AD, Chandra SR. Flavonoids: An overview. J Nutr Sci. 2016;5:47. DOI: 10.1017/jns.2016.41

40. Burak M, Imen Y. Flavonoids and their antioxidant properties. Turkiye Klin Tip Bil Derg. 1999;19:296–304.

41. Madeddu F, Di Martino J, Pieroni M, Del Buono D, Bottoni P, Botta L, Castrignanò T, Saladino R. Molecular docking and dynamics simulation revealed the potential inhibitory activity of new drugs against human topoisomerase I receptor. Int. J. Mol. Sci. 2022;23:14652.
Available:https://doi.org/10.3390/ijms23231465

42. Mahdizade Ari M, Dashtbin S, Ghasemi F, Shahroodian S, kiani P, Bafandeh E, Darbandi T, Ghanavati R, Darbandi A. Nitrofurantoin: properties and potential in treatment of urinary tract infection: a narrative review. Front. Cell. Infect. Microbiol. 2023;13:1148603.
DOI: 10.3389/fcimb.2023.1148603

43. Karplus M, McCammon JA. Molecular dynamics simulations of biomolecules. Nature Structural Biology. 2002;9:646–652.

44. Tomas Hansson, Chris Oostenbrink, WilfredF van Gunsteren. Molecular dynamics simulations. Current Opinion in Structural Biology. 2002;12(2):190–196. DOI:10.1016/s0959-440x(02)00308-1

45. Anwer K, Sonani R, Madamwar D, Singh P, Khan F, Bisetty K, Ahmad F, Hassan MI. Role of N-terminal residues on folding and stability of C-phycoerythrin: simulation and urea-induced denaturation studies, Journal of Biomol Structure Dynamics. 2015;33 (1):121-133.Available:https://doi.org/10.1080/07391102.2013.855144

46. Hubbard RE, Kamran Haider M. Hydrogen bonds in proteins: role and strength. In

eLS; John Wiley & Sons, Ltd.: Hoboken, NJ, USA; 2001.

47. Mohammad T, Siddiqui S, Shamsi A, Alajmi MF, Hussain A, Islam A, Ahmad F, Hassan MI. Virtual Screening Approach to Identify High-Affinity Inhibitors of Serum and Glucocorticoid-Regulated Kinase 1 among Bioactive Natural Products: Combined Molecular Docking and Simulation Studies. *Molecules.* 2020; 25(4):823. https://doi.org/10.3390/molecules25040823

48. Wade RC, Goodford PJ. The role of hydrogen-bonds in drug binding. Prog Clin Biol Res. 1989;289:433-44. PMID: 2726808.

49. Anusuya S, Velmurugan D, Gromiha MM. Identification of dengue viral RNA-dependent RNA polymerase inhibitor using computational fragment based approaches and molecular dynamics study. J. Biomol. Struct. Dyn. 2015;34(7):1512–1532. Available:https://doi.org/10.1080/07391102.2015.1081620

50. Lobanov MY, Bogatyreva NS, Galzitskaya OV. Radius of gyration as an indicator of protein structure compactness. Mol Biol. 2008;42:623–628.Available:https://doi.org/10.1134/S0026893308040195

51. Alfred Rudin, Phillip Choi. The Elements of Polymer Science & Engineering (Third Edition), Science Direct, Elsevier Inc; 2013.

52. Al-Karmalawy AA, Dahab MA, Metwaly AM, Elhady SS, Elkaeed EB, Eissa IH, Darwish KM. Molecular Docking and Dynamics Simulation Revealed the Potential Inhibitory Activity of ACEIs Against SARS-CoV-2 Targeting the *h*ACE2 Receptor. Front Chem. 2021 May 4; 9:661230. DOI: 10.3389/fchem.2021.661230.

53. Veeresham C. Natural products derived from plants as a source of drugs. J Adv Pharm Technol Res. 2012; 3(4): 200. DOI: 10.4103/2231-4040.104709.